AJNR

Sinonasal Organized Hematoma: CT and MR Imaging Findings

E.Y. Kim, H.-J. Kim, S.-K. Chung, H.-J. Dhong, H.Y. Kim, Y.J. Yim, S.T. Kim, P. Jeon and Y.-H. Ko

ORIGINAL RESEARCH

E.Y. Kim
H.-J. Kim
S.-K. Chung
H.-J. Dhong
H.Y. Kim
Y.J. Yim
S.T. Kim
P. Jeon
Y.-H. Ko

Sinonasal Organized Hematoma: CT and MR Imaging Findings

BACKGROUND AND PURPOSE: Sinonasal organized hematoma (OH) is an uncommon, nonneoplastic benign condition that can be locally aggressive. The purpose of this work was to characterize the CT and MR imaging findings of sinonasal OH.

MATERIALS AND METHODS: CT ($n = 11$) and MR ($n = 10$) images of 12 patients (9 men and 3 women; mean age, 41 years; range, 12–76 years) with pathologically proved sinonasal OH were retrospectively reviewed. Particular attention was put on the location, shape, size, extent, internal architecture, and enhancement pattern of the lesion and associated sinus wall change.

RESULTS: The lesions were seen as an expansile ($n = 9$) or nonexpansile ($n = 3$) mass, ranging in size from 2.2 to 6.0 cm (mean, 4.2 cm), primarily involving the maxillary sinus ($n = 11$) or nasal cavity ($n = 1$) unilaterally. The ipsilateral nasal cavity was also involved in 9 of 11 maxillary sinus lesions. Smooth sinus wall erosion other than the medial maxillary sinus wall was noted in 8 lesions. The internal architecture was best displayed on T2-weighted MR images on which all of the lesions were seen as a mixture of marked heterogeneous hypointensity and isointensity, surrounded by a hypointense peripheral rim, reflecting histologic heterogeneity of the lesion composed of hemorrhage, fibrosis, and neovascularization. Marked irregular nodular, papillary, or frondlike enhancement at the areas of neovascularization was also a typical finding seen in all of the lesions.

CONCLUSION: An expansile soft tissue mass, smooth sinus wall erosion, marked heterogeneous signal intensity with a hypointense peripheral rim on T2-weighted MR images, and marked irregular nodular, papillary, or frondlike enhancement are characteristic CT and MR imaging findings of sinonasal OH.

Sinonasal organized hematoma (OH) is an uncommon, nonneoplastic benign condition that can be locally aggressive. Without careful evaluation of all of the imaging features, this may be mistaken for a malignant lesion both clinically and radiologically. It most commonly affects the maxillary sinus and can result from various causes of hemorrhage with chronic hematoma formation, followed by the process of organization through fibrosis and neovascularization.[1,2] Since the first report by Ozhan et al[3] in a patient with von Willebrand disease, only fewer than 40 cases have been reported in the English literature under various names, including pseudotumor,[3,4] hematoma,[5] organized or organizing hematoma,[1,2,6-8] and hematoma-like mass of the maxillary sinus.[9]

Correct preoperative diagnosis of sinonasal OH is important to avoid unnecessary extensive surgery, because this condition is curative with a simple, conservative surgical approach and rarely recurs. Although there have been a few reports on the CT findings of sinonasal OH,[1-3,5-9] which are reported to be rather nonspecific, to our knowledge, the MR imaging features have not systematically been analyzed previously. Only 2 studies had briefly mentioned the MR imaging features.[8,9] Yagisawa et al[9] reported that masses were well demarcated from the surrounding structures and heterogeneous in signal intensity on both T1- and T2-weighted MR images. Song et al[8]

reported that the lesions appeared as isosignal intensity with a margin that had a slightly higher signal intensity on T1-weighted images and a mosaic of various signal intensities and a low signal intensity rim on T2-weighted images. The purpose of this study was to report the CT and MR imaging findings, which are believed to be characteristic for sinonasal OH.

Materials and Methods

Patients

Between July 1995 and June 2007, we experienced 12 patients with pathologically proved sinonasal OH at our institution. The patients included 9 men and 3 women, aged ranging from 12 to 76 years, with a mean age of 41 years. We retrospectively reviewed CT ($n = 11$) and MR ($n = 10$) images obtained in these 12 patients.

Frequent epistaxis and nasal obstruction were the 2 most common chief complaints seen in 7 patients each, followed by rhinorrhea ($n = 2$) and anterior cheek pain ($n = 1$). The duration of symptoms before diagnosis ranged from 1 to 60 months (mean, 14 months). Two patients had a history of previous surgery in the head and neck: one patient underwent endoscopic sinus surgery and uvulopalatopharyngoplasty 5 years ago, and the other patient underwent facial surgery for correction of neurofibromatosis type 1-associated facial anomaly 10 years ago. The latter patient also had coagulation factor V deficiency with a mildly increased prothrombin time (1.4 international normalized ratio obtained at the time of admission). The remaining 11 patients had normal values of coagulation tests. On systemic review, 5 patients had hypertension that had been well controlled by oral medication.

All of the patients underwent surgical removal of OH by using endoscopic sinus surgery ($n = 9$) or Caldwell-Luc operation ($n = 3$). At surgery, most lesions were difficult to remove en bloc because of the surface fragility during surgical manipulation. In no cases were

significant complications encountered in association with surgery. All of the patients were free of disease without evidence of recurrence during the follow-up period of 1–56 months (mean, 19.5 months).

Macroscopically, the OH was seen as a relatively well-circumscribed, lobulated mass with a brown or dark red surface. Microscopically, most of the central areas of the lesion were composed of hemorrhage with fibrin clots, fibrosis, neovascularization, and areas of focal inflammation, surrounded by peripheral attenuated fibrous tissue. In 4 lesions, OH was found to arise in the inflammatory polyp of the sinonasal cavity, including 2 cases of antrochoanal polyp, 1 case of antral polyp, and 1 case of nasal polyp. No case had neoplastic tissue proliferation.

Imaging Techniques

CT scanning was performed in 11 patients and MR imaging in 10 patients. Nine patients underwent both CT and MR examinations. CT scans were obtained by using various models of a spiral CT scanner. Seven patients underwent 2.5- to 3.0-mm-thick axial CT scanning with a soft tissue algorithm both before and after the intravenous administration of a total of 90 mL of iodinated contrast material. In these patients, direct ($n = 2$) or reformatted ($n = 4$) coronal images were also obtained after contrast. In the remaining 4 patients, 3-mm-thick direct axial and coronal scans were obtained with a bone algorithm without the use of contrast material.

MR examinations (10 patients) were performed on a 1.5T ($n = 8$; Signa Advantage Horizon, GE Medical Systems, Milwaukee, Wis) or 3T ($n = 2$; Intera Achieva, Philips, Eindhoven, the Netherlands) scanner. In all patients, precontrast T1-weighted spin-echo images and T2-weighted fast spin-echo images with fat saturation were obtained, followed by contrast-enhanced, T1-weighted spin-echo images with fat saturation after the intravenous injection of 0.1 mmol/kg of gadolinium dimeglumine. Images were obtained in at least 2 planes with 3- to 4-mm section thickness and 0- to 1-mm intersection gap.

Image Analysis

Two neuroradiologists (H.-J.K. and S.T.K.) retrospectively reviewed all of the CT and MR images for consensus. The CT and MR imaging characteristics were analyzed, with particular attention to the location, shape, size, extent, internal architecture, and enhancement pattern of the lesion and change of bony walls of the paranasal sinus. The size of the lesion was measured at the greatest diameter of the lesion. The internal architecture of the lesion was determined by attenuation on precontrast CT scans and signal intensity on T1- and T2-weighted MR images. The presence of calcification within the lesion determined on precontrast CT scans was also recorded. The attenuation and signal intensity of the lesion were compared with those of soft tissue of the inferior turbinate. The degree of enhancement was also subjectively assessed as being mild (enhancement equal to masseter muscle), moderate (enhancement greater than masseter muscle but less than nasal mucosa), or marked (enhancement equal to or greater than nasal mucosa).

Results

The CT and MR imaging features of 12 cases of sinonasal OH were summarized in the On-line Table. On CT and MR images, the lesions were seen as an expansile ($n = 9$) or nonexpansile ($n = 3$) mass, primarily involving the maxillary sinus ($n = 11$) or nasal cavity ($n = 1$) unilaterally (Figs 1–3). The right side was involved in 4 cases and the left side in 8. Although most of the lesions were seen as ill-defined masses on

CT scans, all of the lesions were seen as well-defined masses on MR images. The size of the lesions ranged from 2.2 to 6.0 cm in greatest diameter with a mean of 4.2 cm. Of the 11 lesions primarily involving the maxillary sinus, the ipsilateral nasal cavity was also involved in 9 lesions by nasal obliteration due to the medial wall bulge of the maxillary sinus ($n = 6$; Figs 1 and 2), direct extension into the nasal cavity associated with erosion of the medial wall of the maxillary sinus ($n = 1$), or growth into the nasal cavity through the maxillary sinus ostium in cases associated with an antrochoanal polyp ($n = 2$; Fig 3). One lesion also extended into the adjacent ethmoid sinus. The remaining 2 lesions, including 1 lesion associated with antral polyp, were confined to the maxillary sinus. The lesion primarily involving the nasal cavity was associated with nasal polyp that also extended into the adjacent ethmoid sinus. Smooth, nonaggressive cortical breakthrough and scalloping of the maxillary sinus bony walls beside the medial wall was noted in 8 lesions (66.7%; Figs 1A and 2A). No case showed frank aggressive bone destruction, as seen in a malignant tumor. Focal intralesional calcifications were found on precontrast CT scans in 1 lesion (8.3%).

Compared with soft tissue of the inferior turbinate, the attenuation of the lesion seen on precontrast CT scans obtained in 11 patients was mostly isoattenuated in all, with additional foci of slight hyperattenuation in 8. Compared with the inferior turbinate, all 10 of the lesions examined by MR imaging mostly showed isointensity on T1-weighted images, with additional foci of interspersed hyperintensity in 9 (Fig 1B). In contrast, all of the lesions showed markedly heterogeneous, mixed hypointense, and isointense signal intensity on T2-weighted images, with additional foci of hyperintensity in 3 (Figs 1C, 2C, and 3C). In all of the lesions, T2-weighted images also showed a hypointense peripheral rim surrounding the lesion. Contrast-enhanced CT and MR images demonstrated the areas of moderate ($n = 1$) or marked ($n = 10$) irregular nodular, papillary, or frondlike enhancement in all of the lesions (Figs 1D, 2B, 3A, and 3C). Enhancement occurs roughly at the isointense areas on T2-weighted MR images.

Discussion

Although its pathogenesis is still not clearly understood, sinonasal OH is believed to develop initially from the accumulation of blood in the maxillary sinus resulting from various causes, such as trauma, surgery, bleeding diatheses, hemorrhagic lesion within the sinus, and the loss of mechanical integrity of an arterial branch, as seen in a ruptured aneurysm or inflammatory erosion of an arterial wall.[1,2,5-7] OH occurs most frequently in the maxillary sinus, because the maxillary sinus is the largest paranasal sinus that allows conditions of negative pressure and decreased ventilation.[2] Regardless of the initial cause of bleeding, poor ventilation and drainage with the aid of the formation of a fibrous capsule prevent reabsorption of the hematoma and result in neovascularization and fibrosis with recurrent intracapsular bleeding, leading to the eventual formation of OH. This process accounts for progressive expansion and local bony erosion associated with OH.[1-3,5-7] In this study, 2 of 12 patients had a history of previous surgery in the head and neck. One of these 2 patients also had coagula-
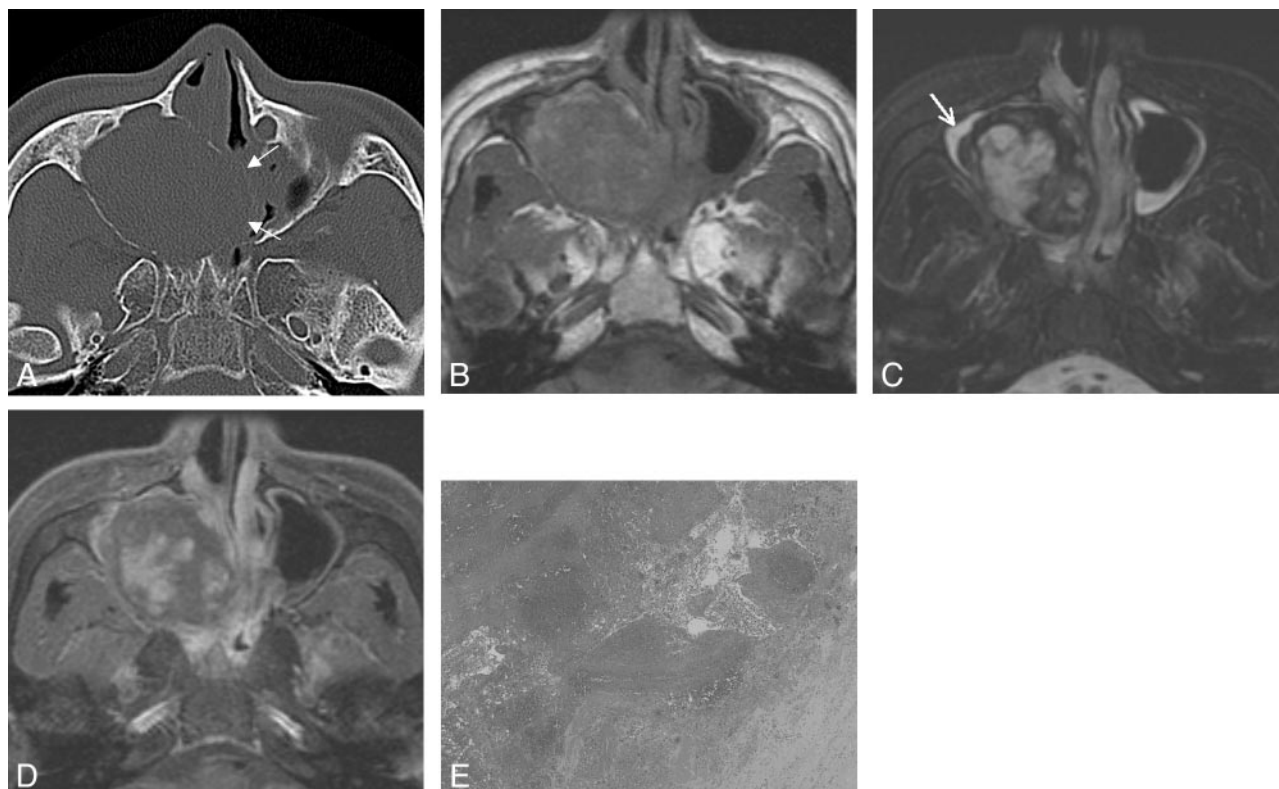
Fig 1. Case 5. Organized hematoma of the maxillary sinus in a 50-year-old man. *A,* Precontrast axial CT scan with bone algorithm shows a large, expansile soft tissue mass in the right maxillary sinus with cortical thinning and scalloping of bony walls of the maxillary sinus. The ipsilateral nasal cavity is occluded by the lesion that pushes the medial maxillary sinus wall and nasal septum contralaterally (*arrows*). *B,* Axial T1-weighted MR image shows that the lesion is mostly isointense to the inferior turbinate interspersed with foci of hyperintensity. *C,* Axial, fat-suppressed, T2-weighted MR image shows the marked heterogeneity of the lesion with a mix of hypointense, isointense, and hyperintense signals. A dark peripheral rim surrounding the lesion is also well demonstrated. Note a bright signal intensity due to mucosal inflammation of the involved maxillary sinus (*arrow*), which is nicely distinguished from the lesion on T2-weighted images. *D,* Contrast-enhanced axial, fat-suppressed, T1-weighted MR image shows a marked frondlike, papillary enhancement within the lesion, roughly at the isointense areas on the T2-weighted image. *E.* Photomicrograph shows that the lesion consists mostly of extravasated red blood cells and prominent fibrosis (hematoxylin-eosin, original magnification, ×400).


Fig 2. Case 10. Organized hematoma of the maxillary sinus in a 76-year-old woman. *A,* Precontrast axial CT scan with bone window setting shows a large, expansile soft tissue mass in the right maxillary sinus, which causes cortical thinning and scalloping of bony walls of the maxillary sinus (*arrows*). With soft tissue windowing, the lesion is isoattenuated to the inferior turbinate with focal hyperattenuated area (data not shown). *B,* Contrast-enhanced axial CT scan shows marked irregular linear and nodular enhancement within the lesion. Note focal effacement of the retromaxillary fat by the expansile mass that causes smooth erosion of the sinus wall (*arrow*). *C,* Axial, fat-suppressed, T2-weighted MR image shows marked heterogeneity of the lesion composed of the areas of hypointensity and isointensity compared with the inferior turbinate. A dark peripheral rim surrounding the lesion is also well demonstrated.

tion factor V deficiency and showed a mildly increased prothrombin time.

Clinically, symptoms do not usually occur while the lesion remains localized to the maxillary sinus. Because there is gradual enlargement of the lesion causing erosion and displacement of the adjacent bony structures, symptoms such as epistaxis, cheek swelling, nasal obstruction, and exophthalmos become manifest.[9] In this series, like others reported previ-

ously, frequent epistaxis and nasal obstruction also were the 2 most common symptoms seen in 7 patients each, followed by rhinorrhea and perinasal pain. A wide age range has been reported from 11 to 78 years, with the male-to-female ratio of 2–3:1.[3,6,8,9] In the present study, patients' age ranged from 12 to 76 years (mean, 41 years), and there was a predilection for men, with the male-to-female ratio of 3:1. The reported clinical course before diagnosis was also variable. Lee et al[2] re-
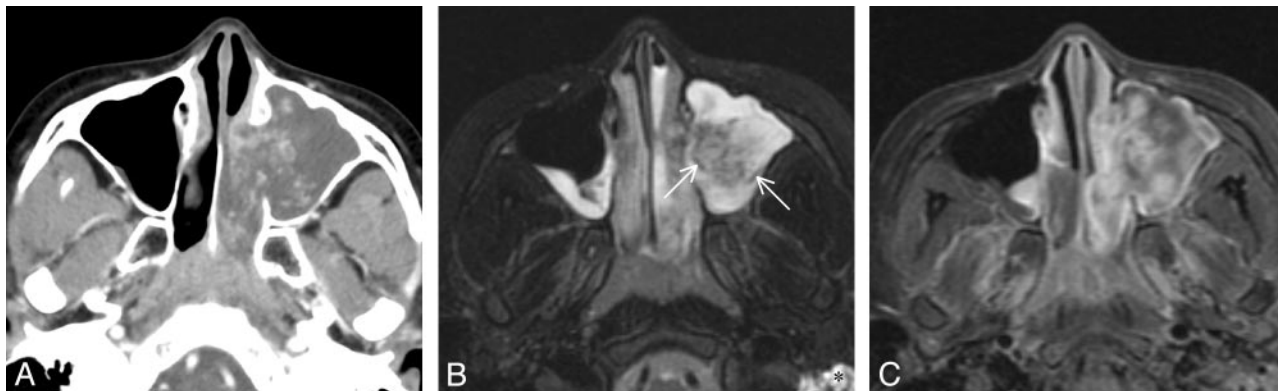
Fig 3. Case 2. Organized hematoma arising from antrochoanal polyp in a 12-year-old girl. *A,* Contrast-enhanced axial CT scan shows marked irregular nodular enhancement within a mass in the left maxillary sinus, which protrudes into the ipsilateral posterior nasal cavity through the widened maxillary sinus ostium. *B,* Axial, fat-suppressed, T2-weighted MR image reveals that the lesion is mixed hypointense and isointense to the inferior turbinate and is located inside the hyperintense antrochoanal polyp occupying the entire left maxillary sinus and posterior nasal cavity. Scattered foci of dark peripheral rim surrounding the lesion are also well demonstrated (*arrows*). Note the opacified ipsilateral mastoid air cells (*) caused by Eustachian tube obstruction by nasopharyngeal extension of the antrochoanal polyp. *C,* Contrast-enhanced axial, fat-suppressed, T1-weighted MR image shows the large areas of marked papillary enhancement within the lesion.

ported 3 months of the mean duration of symptoms before diagnosis (range, 2–13 months). In this study, it was 14 months (range, 1–60 months).

Correct preoperative diagnosis is important for determining the therapeutic plans, because sinonasal OH is usually curative with complete surgical resection simply by using endoscopic sinus surgery or Caldwell-Luc operation.[2,7,8] However, locally aggressive behavior caused by increasing pressure within the hematoma can lead to erosion of the sinus walls, thus making differentiation from the locally aggressive lesion difficult on the clinical basis alone.

The reported CT appearances of sinonasal OH are rather nonspecific, and typically include a large mass causing expansion of the maxillary sinus with bony erosion and heterogeneous high attenuation on precontrast CT scans.[2,7,8] Although there are different opinions about the enhancing characteristics on contrast-enhanced CT scans, patchy heterogeneous enhancement with various degrees is usually found within the lesion.[2]

In the present study, CT and MR imaging provided the important information on the characteristics of the lesions to make the correct diagnosis. Nine (75%) of the 12 lesions were expansile with the frequent association of smooth, nonaggressive cortical breakthrough and scalloping of the maxillary sinus walls beside the medial wall, noted in 8 (66.7%). The expansion pattern was never invasive, as seen in malignancy. CT was superior to MR imaging for demonstrating this kind of benign bone changes associated with the lesion. It was also better than MR imaging in the detection of calcification, which was seen in 1 lesion (8.3%) in this study. According to Lee et al,[2] compared with masticator muscle, the attenuation of OH on precontrast CT scans obtained in 8 patients was heterogeneously hyperattenuated in 5 and isoattenuated in 3. Likewise, all of our 11 lesions examined with precontrast CT scans were seen as isoattenuated to soft tissue of the inferior turbinate, with additional foci of slight hyperattenuation in 8.

In this study, MR imaging was superior to CT for determining the margin and extent of the lesion. Although most of the lesions were seen as ill-defined masses on CT scans, all of the lesions were seen as a well-defined masses on MR images.

In addition, the opacities of the adjacent paranasal sinuses caused by secondary obstruction and inflammation could be differentiated easily from the lesion on MR images, especially on T2-weighted images (Fig 1*C*). Furthermore, due to the higher soft tissue contrast resolution, MR imaging better showed the internal characteristics of the lesion by demonstrating various signal intensities on T1- and T2-weighted images. Although an exact 1:1 MR-pathologic correlation could not be performed because most lesions were removed in pieces and not en bloc, we believe that the heterogeneous signal intensity seen on MR images reflects the various components contained within the lesion, such as hemorrhage in various stages, fibrosis, and various amounts of vascular proliferation. As described by Song et al,[8] a hypointense peripheral rim was also demonstrated on T2-weighted images in all of the lesions, which corresponded histologically with an attenuated fibrous pseudocapsule.

As expected, MR imaging was more sensitive to the presence of contrast enhancement than CT. The areas of enhancement roughly corresponded with those of isointensity on T2-weighted MR images. We believe that enhancement is attributed to neovascularization, as suggested by Lee et al,[2] and also that the isointense areas seen on T2-weighted images, therefore, represent the areas of prominent vascular proliferation.

Interestingly, in 4 of our 12 lesions, the OH was found within the inflammatory sinonasal polyp: 2 within the antrochoanal polyp; 1 within the antral polyp; and the remaining 1 within the nasal polyp. We postulate that OH associated with a sinonasal polyp may be a special form of angiomatous polyp, which is a rare disease entity of which the pathogenesis is not clearly understood.[10-13] It is considered a subtype of inflammatory sinonasal polyps, characterized histologically by extensive vascular proliferation and ectasis.[13] Regardless of the exact pathogenesis of the angiomatous polyp, the similarities of reported CT and MR imaging features of an angiomatous polyp with those of 4 cases of OH formed within the sinonasal polyp in this study suggest that these 2 might represent the same disease entities.[10,12,13]

In addition to OH, there is a long list of the differential

diagnoses of a unilateral mass in the sinonasal cavity detected on CT and MR images, including mucocele, fungus ball, inflammatory polyp, cholesterol granuloma, inverted papilloma, hemangioma, and carcinoma.[2,6,8] Administration of contrast material is extremely useful, because mucocele, fungus ball, inflammatory polyp, and cholesterol granuloma do not usually enhance. Inverted papilloma primarily involves the nasal cavity and shows the rather characteristic convoluted cerebriform pattern on T2- or enhanced T1-weighted MR images.[14] Sinonasal hemangioma, especially the cavernous type, is probably the most difficult lesion to differentiate from OH both clinically and radiologically. Although Yagisawa et al[9] suggested that hemangioma and sinonasal OH be the same pathologic entity, the fact that the vascular lumina of cavernous hemangioma are usually larger than those of OH on histologic examination still raises the probable different nature of the 2 lesions. Frank bony destruction, rather than smooth erosion of the sinus walls, associated with adjacent tissue invasion is a hallmark of carcinoma.[2]

Conclusions

Although rare, sinonasal OH may be mistaken for a malignant or locally aggressive neoplasm by presenting as an expansile soft tissue mass with erosion of the adjacent sinus walls. CT and MR images demonstrated quite characteristic findings, including an expansile soft tissue mass, smooth erosion of bony sinus walls, marked heterogeneous signal intensity with a peripheral rim of hypointensity on T2-weighted MR images, and marked patchy, papillary, or frondlike enhancement on contrast-enhanced CT and MR images.

References

1. Lee BJ, Park HJ, Heo SC. **Organized hematoma of the maxillary sinus**. *Acta Otolaryngol* 2003;123:869–72
2. Lee HK, Smoker WR, Lee BJ, et al. **Organized hematoma of the maxillary sinus: CT findings.** *AJR Am J Roentgenol* 2007;188:W370–73
3. Ozhan S, Arac M, Isik S, et al. **Pseudotumor of the maxillary sinus in a patient with von Willebrand's disease.** *AJR Am J Radiol* 1996;166:950–51
4. Steele NP, Myssiorek D, Zahtz GD, et al. **Pediatric hemophilic pseudotumor of the paranasal sinus.** *Laryngoscope* 2004;114:1761–63
5. Tabaee A, Kacker A. **Hematoma of the maxillary sinus presenting as a mass–a case report and review of literature.** *Int J Pediatr Otorhinolaryngol* 2002;65:153–57
6. Unlu HH, Mutlu C, Ayhan S, et al. **Organized hematoma of the maxillary sinus mimicking tumor.** *Auris Nasus Larynx* 2001;28:253–55
7. Yoon TM, Kim JH, Cho YB. **Three cases of organized hematoma of the maxillary sinus.** *Eur Arch Otorhinolaryngol* 2006;263:823–26
8. Song HM, Jang YJ, Chung Y-S, et al. **Organizing hematoma of the maxillary sinus.** *Otolaryngol Head Neck Surg* 2007;136:616–20
9. Yagisawa M, Ishitoya J, Tsukuda M. **Hematoma-like mass of the maxillary sinus.** *Acta Otolaryngol* 2006;126:277–81
10. Som PM, Cohen BA, Sacher M, et al. **The angiomatous polyp and the angiofibroma: two different lesions.** *Radiology* 1982;144:329–34
11. Batsakis JG, Seige N. **Choanal and angiomatous polyps of the sinonasal tract.** *Ann Oatol Rhinol Laryngol* 1992;101:623–25
12. De Vuysere S, Hermans R, Marchal G. **Sinochoanal polyp and its variant, the angiomatous polyp: MRI findings.** *Eur Radiol* 2001;11:55–58
13. Sheahan P, Crotty PL, Hamilton S, et al. **Infarcted angiomatous nasal polyps.** *Eur Arch Otorhinolaryngol* 2005;262:225–30
14. Ojiri H, Ujita M, Tada S, et al. **Potentially distinctive features of sinonasal inverted papilloma on MR imaging.** *AJR Am J Roentgenol* 2000;175:465–68